

This article was downloaded by: [Chongqing University]

On: 14 February 2014, At: 13:30

Publisher: Taylor & Francis

Informa Ltd Registered in England and Wales Registered Number: 1072954 Registered office: Mortimer House, 37-41 Mortimer Street, London W1T 3JH, UK



Journal of Coordination Chemistry

Publication details, including instructions for authors and subscription information:

<http://www.tandfonline.com/loi/gcoo20>

Cu(II) complexes of a new tetradentate N₂SO donor: synthesis, structure, electrochemistry, and DFT computation

Ajoy Kumar Pramanik^a, Mahendra Sekhar Jana^a & Tapan Kumar Mondal^a

^a Department of Chemistry, Inorganic Chemistry Section, Jadavpur University, Kolkata, India

Accepted author version posted online: 23 Oct 2013. Published online: 04 Dec 2013.

To cite this article: Ajoy Kumar Pramanik, Mahendra Sekhar Jana & Tapan Kumar Mondal (2013) Cu(II) complexes of a new tetradentate N₂SO donor: synthesis, structure, electrochemistry, and DFT computation, Journal of Coordination Chemistry, 66:23, 4067-4079, DOI: [10.1080/00958972.2013.857407](https://doi.org/10.1080/00958972.2013.857407)

To link to this article: <http://dx.doi.org/10.1080/00958972.2013.857407>

PLEASE SCROLL DOWN FOR ARTICLE

Taylor & Francis makes every effort to ensure the accuracy of all the information (the "Content") contained in the publications on our platform. However, Taylor & Francis, our agents, and our licensors make no representations or warranties whatsoever as to the accuracy, completeness, or suitability for any purpose of the Content. Any opinions and views expressed in this publication are the opinions and views of the authors, and are not the views of or endorsed by Taylor & Francis. The accuracy of the Content should not be relied upon and should be independently verified with primary sources of information. Taylor and Francis shall not be liable for any losses, actions, claims, proceedings, demands, costs, expenses, damages, and other liabilities whatsoever or howsoever caused arising directly or indirectly in connection with, in relation to or arising out of the use of the Content.

This article may be used for research, teaching, and private study purposes. Any substantial or systematic reproduction, redistribution, reselling, loan, sub-licensing, systematic supply, or distribution in any form to anyone is expressly forbidden. Terms &



Cu(II) complexes of a new tetradentate N₂SO donor: synthesis, structure, electrochemistry, and DFT computation

AJOY KUMAR PRAMANIK, MAHENDRA SEKHAR JANA and
TAPAN KUMAR MONDAL*

Department of Chemistry, Inorganic Chemistry Section, Jadavpur University, Kolkata, India

(Received 8 April 2013; accepted 20 September 2013)

Cu(II) complexes having distorted square pyramidal geometry with N₂SO donor azo–thioether ligand, [Cu(L)X] (X = Cl (**1**) and Br (**2**)), have been synthesized and characterized. The geometries of the complexes are confirmed by single crystal X-ray analysis. The complexes form supramolecular 1D chains by intermolecular H-bonding and π – π interaction between the pyridines. Spectral and electrochemical properties have been studied. Electronic structure and spectral properties are explained by DFT and TDDFT analysis.

Keywords: Cu(II) complexes; N₂SO donor azo–thioether ligand; X-ray structure; DFT computation

1. Introduction

Azo dyes are important colorants consisting of at least a conjugated azo (–N=N–) chromophore. The color of azo compounds depends on the nature of both the diazo and coupling components. Structural diversities exhibited by arylazo compounds containing active methylene groups such as 1,3-diketones have developed immense interest during the last few decades [1, 2]. The structural diversity, redox property, and antibacterial activities of Cu(II) and Ni(II) complexes with N,N,O donor thioether containing arylazo compounds with 1,3-diketones have been reported elsewhere [3, 4].

Chelating ligands containing N, S, and/or O donor atoms have broad biological activity and have unique interest in coordination chemistry because of the stability, chemical and electrochemical activities, and diversity in binding to metal ions [5–13]. The transition metal complexes of these ligands have been extensively studied because of their potential antimicrobial [14–17], antioxidant [18], anticancer, and catalytic activities [19–22]. Polydentate ligands with thioether moieties are often used for synthesis of model complexes to mimic the spectroscopic and structural properties of the active sites of metallo proteins [23–26].

In recent years, several reports have appeared pertaining to the models of copper enzymes. The potential role played by copper(II), being present in the active site of a large number of metalloproteins [27], has encouraged us to design a new ligand frame having

*Corresponding author. Email: tkmondal@chemistry.jdvu.ac.in

nitrogen, sulfur, and oxygen donor centers, and to study the electrochemical, molecular, and electronic structural aspects of its Cu(II) complexes.

In this work, we have synthesized thioether containing a new N₂SO donor arylazo ligand (HL) and its isostructural square pyramidal Cu(II) complexes having the general formula [Cu(L)X] [where X = Cl (**1**) and Br (**2**)], keeping in mind that the square pyramidal Cu(II) complexes show antibacterial and antioxidant activities, potentially bound with DNA and form supramolecular geometry within the structure [28–36]. The geometries of the present complexes have been confirmed by single crystal X-ray study and show distorted square pyramidal geometry around Cu(II). The complexes form supramolecular structures by potential intermolecular H-bonding and π – π^* interactions. Electronic structure and electrochemical properties of the complexes have been supported by DFT calculation. TDDFT calculation has been used to simulate the experimental electronic spectra of the complexes.

2. Experimental

2.1. Materials and methods

2-((Pyridine-2-yl)methylthio)benzenamine was prepared following the reported procedure [37]. 2-Aminothiophenol and 2-(chloromethyl)pyridine were purchased from Sigma Aldrich. All other chemicals and solvents were of reagent grade and used as received.

Microanalyses (C, H, and N) were performed using a Perkin-Elmer CHN-2400 elemental analyzer. The electronic spectra were measured on a Lambda 25 Perkin-Elmer spectrophotometer in acetonitrile solution. The IR spectra were recorded on a RX-1 Perkin-Elmer spectrometer from 4000 to 400 cm^{–1} with the samples in the form of KBr pellets. ¹H NMR spectrum of HL was recorded in CDCl₃ on a Bruker 300 MHz FT-NMR spectrometer in the presence of TMS as internal standard. The magnetic measurements of the complexes were done using the Gouy method. ESI mass spectra were recorded on a micro mass Q-TOF mass spectrometer. EPR spectra in the X band were recorded with a JEOL JES-FA200 spectrometer. Cyclic voltammetric measurements were carried out using a CHI Electrochemical workstation. A platinum wire working electrode, a platinum wire auxiliary electrode, and Ag/AgCl reference electrode were used in a standard three-electrode configuration. [nBu₄N][ClO₄] was used as supporting electrolyte and the scan rate used was 50 mV s^{–1} in acetonitrile under dinitrogen atmosphere. Molar conductances were measured using Systronics conductivity meter (Model 304) using ca. 10^{–3} M solutions in acetonitrile.

2.2. Synthesis of ligand, HL

2-((Pyridine-2-yl)methylthio)benzenamine (1.730 g, 8 mM) was dissolved in 8 mL conc. HCl. The ice cold NaNO₂ (0.622 g, 9 mM) solution was added dropwise to the ice cold amine solution under stirring condition and resulting solution was kept in an ice bath. It was then added to an ice cold solution of acetylacetone (0.801 g, 8 mM) dissolved in Na₂CO₃ (10.612 g) under vigorous stirring condition. A yellow precipitate of the ligand was obtained. The crude product was collected by filtration. The crude product was dissolved in 100 mL 1(M) HCl and filtered; the filtrate was neutralized with dilute Na₂CO₃ solution for re-precipitation of the compound. The precipitate was collected by filtration, washed with distilled water, and dried over CaCl₂. Yield was 1.972 g, (75%); m.p. 72 °C.

Microanalytical data: Anal. Calcd for $C_{17}H_{18}N_3O_2S$: C, 62.36; H, 5.23; N, 12.83. Found (%): C, 62.57; H, 5.27; N, 12.91%. IR data (KBr disk) (cm^{-1}): 3430 $\nu(\text{O-H})$, 2926 $\nu(\text{C-H})$, 1677 $\nu(\text{C=O})$, 1577 $\nu(\text{C=N})$, 1505 $\nu(\text{C=C})$, 1433 $\nu(\text{N=N})$. ^1H NMR data in CDCl_3 (δ , ppm): 15.10 (s, 1H), 8.43 (d, $J = 5.2$ Hz, 1H), 7.73 (d, $J = 8.2$ Hz, 1H), 7.54 (t, $J = 8.5$ Hz, 1H), 7.34–7.40 (m, 2H), 7.16 (d, $J = 7.8$ Hz, 1H), 7.04–7.10 (m, 2H), 4.11 (s, 3H), 2.62 (s, 3H), 2.48 (s, 3H). λ_{max} (ϵ , $\text{M}^{-1} \text{cm}^{-1}$) in acetonitrile: 403 (sh), 368 (21086), 255 (17210). ESI-MS, m/z : 328 $[\text{MH}]^+$.

2.3. Synthesis of complexes

2.3.1. Preparation of $[\text{Cu}(\text{L})\text{Cl}]$ (1). To a 15 mL methanolic solution of HL (0.251 g, 0.764 mM), 10 mL methanolic solution of $\text{CuCl}_2 \cdot 2\text{H}_2\text{O}$ (0.123 g, 0.722 mM) was added dropwise under stirring condition. The stirring was continued for 1 h and then refluxed for 4 h. The resultant deep brown solution was kept for slow evaporation of the solvent. After a week, the brown crystal suitable for single X-ray crystal study of the complex was found. Yield was 0.227 g, 74%.

Microanalytical data: Anal. Calcd for $C_{17}H_{16}\text{ClCuN}_3\text{O}_2\text{S}$: C, 48.00; H, 3.79; N, 9.88. Found: C, 48.27; H, 3.81; N, 9.92%. IR data (KBr disk) (cm^{-1}): 1662 $\nu(\text{C=O})$, 1542 $\nu(\text{C=N})$, 1406 $\nu(\text{N=N})$. λ_{max} (ϵ , $\text{M}^{-1} \text{cm}^{-1}$) in acetonitrile: 686 (239), 527 (469), 411 (24028), 285 (25185), 262 (30386). ESI-MS, m/z : 425 $[\text{MH}]^+$.

2.3.2. Synthesis of $[\text{Cu}(\text{L})\text{Br}]$ (2). To a 15 mL methanolic solution of HL (0.215 g, 0.654 mM), CuBr_2 solution (0.145 g, 0.650 mM, in 10 mL methanol) was added dropwise under stirring condition. The stirring was continued for 1 h and then refluxed for 6 h. The resultant brown solution was kept for slow evaporation of the solvent. After a week, the brown crystal suitable for single X-ray crystal study of the complex was found. Yield was 0.221 g, 72%.

Microanalytical data: Anal. Calcd for $C_{17}H_{16}\text{ClCuN}_3\text{O}_2\text{S}$: C, 43.46; H, 3.43; N, 8.94. Found: C, 43.62; H, 3.45; N, 8.97%. IR data (KBr disk) (cm^{-1}): 1661 $\nu(\text{C=O})$, 1535 $\nu(\text{C=N})$, 1405 $\nu(\text{N=N})$. λ_{max} (ϵ , $\text{M}^{-1} \text{cm}^{-1}$) in acetonitrile: 683 (376), 534 (754), 412 (24096), 388 (21566), 269 (40104). ESI-MS, m/z : 469 $[\text{MH}]^+$.

2.4. X-ray crystallography

The crystals, $[\text{Cu}(\text{L})\text{Cl}]$ (1) and $[\text{Cu}(\text{L})\text{Br}]$ (2), were grown by slow evaporation of the reaction mixture in methanol over a week. Data were collected (table 1) using a Bruker AXS Kappa Apex-II diffractometer equipped with an Apex-II CCD area detector using graphite monochromated $\text{Mo K}\alpha$ radiation (0.71073 Å). Reflection data were recorded using the ω scan technique. Unit cell parameters were determined from least-squares refinement of setting angles with θ in the range $1.78 \leq \theta \leq 27.61^\circ$ and $2.25 \leq \theta \leq 27.05^\circ$ for **1** and **2**, respectively. Out of 14,809 collected data 41,836 with $I > 2\sigma(I)$ within the $-9 \leq h \leq 10$, $-14 \leq k \leq 14$, $-15 \leq l \leq 15$ for **1** and out of 14,536 collected data 4181 with $I > 2\sigma(I)$ within the $-10 \leq h \leq 10$, $-14 \leq k \leq 14$, $-15 \leq l \leq 15$ for **2** were used for structure solution. The structures were solved and refined by full-matrix least-squares on F^2 using SHELXS-97 [38]. The absorption corrections were done by the multiscan technique.

Table 1. Crystal data and details of the structure determinations of **1** and **2**.

	[Cu(L)Cl] (1)	[Cu(L)Br] (2)
Formula	C ₁₇ H ₁₆ ClCuN ₃ O ₂ S	C ₁₇ H ₁₆ BrCuN ₃ O ₂ S
Formula weight	425.38	469.84
Crystal system	Triclinic	Triclinic
Space group	<i>P</i> −1	<i>P</i> −1
<i>a</i> (Å)	7.7746(3)	7.789(5)
<i>b</i> (Å)	11.0128(4)	10.956(5)
<i>c</i> (Å)	12.1177(4)	12.220(5)
α (°)	70.808(2)	106.123(5)
β (°)	86.312(2)	93.923(5)
γ (°)	69.576(2)	110.340(5)
<i>V</i> (Å ³)	916.77(6)	923.4(8)
<i>Z</i>	2	2
ρ (Calcd) (g/cm ³)	1.541	1.690
μ (Mo K α) (mm ^{−1})	1.466	3.474
<i>F</i> (0 0 0)	434	470
Crystal size (mm)	0.28 × 0.22 × 0.20	0.36 × 0.28 × 0.24
<i>T</i> (K)	293(2)	293(2)
Radiation wavelength (Å)	0.71073	0.71073
θ (Min–Max) (°)	1.78–27.61	1.76–27.49
<i>h k l</i> Range	−9 to 10; −14 to 14; −15 to 15	−10 to 10; −14 to 14; −15 to 15
Total, unique data, <i>R</i> (int)	14,809, 4183, 0.0284	14,536, 4181, 0.0562
Observed data (<i>I</i> > 2 σ (<i>I</i>))	3462	3152
<i>N</i> _{ref} , <i>N</i> _{par}	4183, 226	4181, 226
<i>R</i> ^a , <i>wR</i> ₂ ^b , <i>S</i> ^c	0.0363, 0.1144, 1.077	0.0478, 0.1521, 0.984
Residual density (e/Å ³)	−0.342 and 0.949	−1.053 and 0.617

^a $R_1 = \sum [|F_o| - |F_c|] / \sum |F_o|$.
^b $wR_2 = \{ \sum [w(F_o^2 - F_c^2)^2] / \sum [w(F_o^2)^2] \}^{1/2}$, $w = 1/[\sigma^2(F_o^2) + (0.0686 P)^2 + 0.1985 P]$ for **1** and $w = 1/[\sigma^2(F_o^2) + (0.0420 P)^2 + 0.9842 P]$ for **2**, where $P = (F_o^2 + 2 F_c^2)/3$.
^cGOF (*S*) = $\{ \sum [w(F_o^2 - F_c^2)^2] / (n - p) \}^{1/2}$, where *n* = number of measured data and *p* = number of parameters.

All data were corrected for Lorentz and polarization effects, and the nonhydrogen atoms were refined anisotropically. Hydrogens were generated using SHELXL-97 [38] and their positions were calculated based on the riding mode with thermal parameters equal to 1.2 times that of associated C atoms, and participated in the calculation of the final *R* indices.

2.5. Computational methods

All computations were performed using the Gaussian03 (G03) program [39]. Full geometry optimizations of **1** and **2** were carried out using the DFT method at the UB3LYP level of theory [40, 41]. The 6–31G(d) basis set for C, H, N, and O atoms and 6–311G(d) basis set for S, Cl, and Br atoms were used. The lanL2TZ(f) basis set with effective core potential was employed for the Cu atom [42]. The lanL2TZ(f) basis set for Cu was downloaded from EMSL basis set library. The vibrational frequency calculations were performed to ensure that the optimized geometries represent the local minima of potential energy surface and there are only positive eigenvalues. The lowest 40 singlet – singlet vertical electronic excitations based on B3LYP optimized geometries were computed using the time-dependent density functional theory (TD-DFT) formalism [43–45] in acetonitrile using conductor-like polarizable continuum model (CPCM) [46–48] using the same B3LYP level and basis sets. GaussSum [49] was used to calculate the fractional contributions of various groups to each molecular orbital.

3. Results and discussion

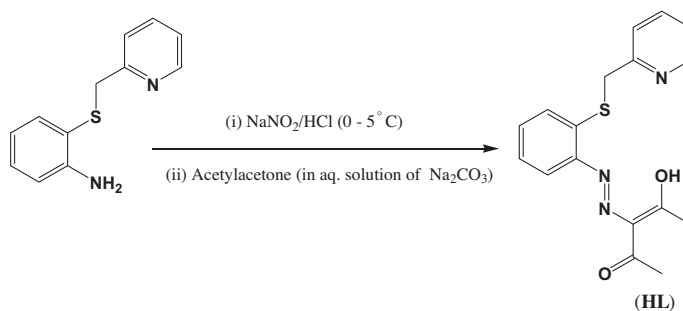
3.1. Synthesis and formulation

The new N_2SO donor arylazo ligand HL is prepared by diazo-coupling reaction between 2-((pyridine-2-yl)methylthio)benzenamine and acetylacetone in aqueous Na_2CO_3 medium (scheme 1). The ligand is characterized by 1H NMR and elemental analysis. The 1H NMR signals in $CDCl_3$ well supported the proposed structure of HL. Two sharp singlets for ketonic and enolic $-CH_3$ protons appeared at 2.51 and 2.48 ppm. The 1-H proton adjacent to pyridyl-N is a weakly coupled doublet at 8.42 ppm ($J = 4.81$ Hz). The characteristic singlet peak corresponds to $-OH$ proton appearing at 15.10 ppm. Other aromatic protons appear at 7.05–7.71 ppm. IR spectrum of HL shows characteristic $\nu(O-H)$, $\nu(C=O)$, 1577 $\nu(C=N)$, and 1433 $\nu(N=N)$ at 3430, 1677, 1577, and 1433 cm^{-1} , respectively.

HL has been used to synthesize new Cu(II) complexes having the general formula $[Cu(L)Cl]$ (**1**) and $[Cu(L)Br]$ (**2**) by reaction with $CuCl_2 \cdot 2H_2O$ and $CuBr_2$, respectively, in methanol. The complexes have been characterized by elemental and spectral analysis. The $\nu(C=N)$ and $\nu(N=N)$ stretching in the complexes are significantly red shifted compared to the free ligands and observed at 1542 and 1406 cm^{-1} , respectively, for **1** and 1335 and 1405 cm^{-1} , respectively, in **2**, suggesting coordination of azo-N and pyridyl-N to Cu(II). The pseudo-square pyramidal geometries of the complexes have been confirmed from single crystal X-ray structures. To know the structural features of the complexes in solution, conductivity measurements were carried out. The complexes behave as nonelectrolytes ($\lambda_M = 4-6 \Omega^{-1} M^{-1} cm^2$) in acetonitrile solution, suggesting the retention of the structure in solution.

3.2. Molecular structure

The ORTEP views with the atom numbering scheme of **1** and **2** are shown in figures 1 and 2, respectively. Detailed crystallographic data are given in table 1. Some selected bond distances and angles are given in table 2. In the isostructural complexes **1** and **2**, the ligand is coordinated through pyridyl-N, thioether-S, azo-N, and enolic-O to the central Cu atom (Cu1), while the fifth coordination site of the distorted square pyramidal geometry has been occupied by Cl and Br in **1** and **2**, respectively. In both complexes, the geometry around the copper(II) ion can be best described as trigonal bipyramidal distorted square based



Scheme 1. Synthesis of HL.

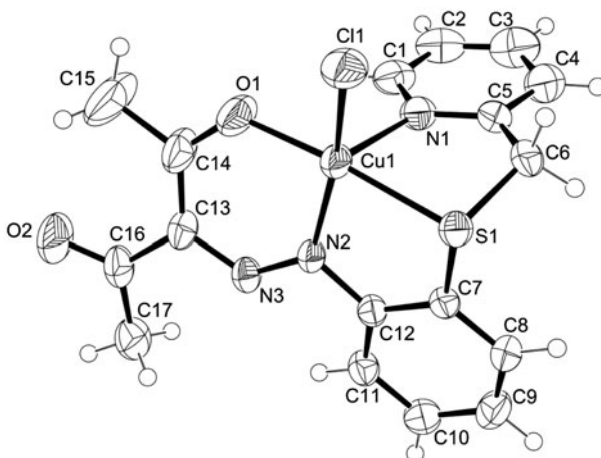


Figure 1. Molecular structure of **1** with 50% ellipsoidal probability.

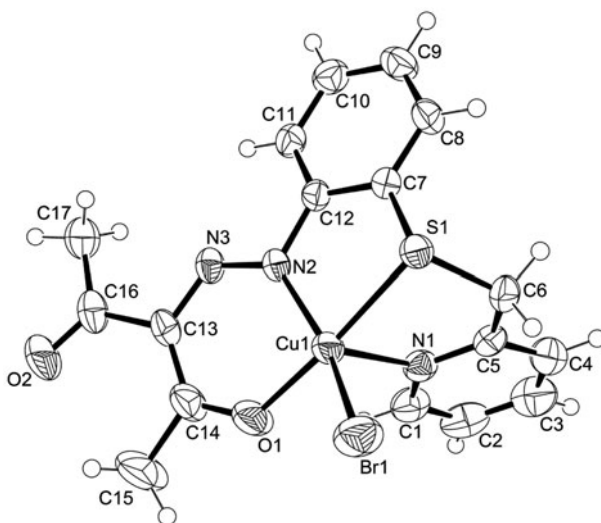


Figure 2. Molecular structure of **2** with 50% ellipsoidal probability.

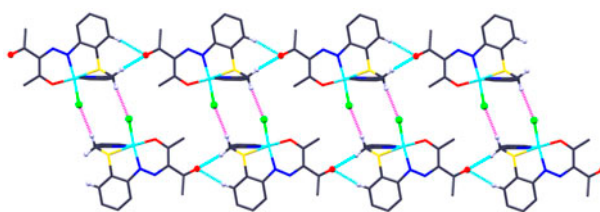
pyramidal (TBSBP) as indicated by the value of the trigonal index $\tau = 0.25$ for **1** and 0.31 for **2** ($\tau = (\beta - \alpha)/60$), where α and β are the largest coordination angles. The value of τ is 1 for perfect trigonal bipyramidal geometry and is zero for a perfect square pyramidal geometry [50]. The equatorial Cu–N(azo) bond distances are much shorter (Cu1–N2, $1.958(2)$ in **1** and $1.954(3)$ Å in **2**) compared to the axial Cu–N(pyridyl) distances (Cu1–N1, $2.256(2)$ and $2.251(4)$ Å in **1** and **2**, respectively), suggesting elongation of the axial bond in the distorted square pyramidal geometry and $d\pi(\text{Cu}) \rightarrow \pi(\text{N}=\text{N})$ back donation in the complexes (table 2). The structural features of the present compounds are very similar to the reported square pyramidal Cu(II) complexes [51]. The atomic arrangement Cu1–S1–C6–C5–N1 (Cg(1)), Cu1–S1–C7–C12–N2 (Cg(2)), and Cu1–O1–C14–C13–N3–N2 (Cg(3)) constitute

Table 2. Selected bond distances (Å) and angles (°) of **1** and **2**.

	1 (X = Cl)		2 (X = Br)	
	X-ray	Calcd	X-ray	Calcd
Bonds (Å)				
Cu1–N1	2.256(2)	2.296	2.251(4)	2.285
Cu1–N2	1.958(2)	1.982	1.954(3)	1.997
Cu1–O1	1.9345(16)	1.978	1.924(3)	1.982
Cu1–X1	2.2589(7)	2.281	2.3858(11)	2.417
Cu1–S1	2.3182(6)	2.374	2.3113(14)	2.361
N2–N3	1.288(3)	1.288	1.293(4)	1.288
N3–C13	1.340(3)	1.339	1.353(5)	1.339
O1–C14	1.252(3)	1.257	1.258(5)	1.258
O2–C16	1.209(3)	1.225	1.212(5)	1.225
C13–C14	1.435(4)	1.455	1.418(6)	1.454
C13–C16	1.484(4)	1.490	1.490(5)	1.489
Angles (°)				
N1–Cu1–N2	94.93(8)	94.84	96.43(13)	95.89
N1–Cu1–O1	100.40(10)	102.7	98.83(16)	100.7
N1–Cu1–S1	81.38(5)	81.03	81.76(10)	81.13
N1–Cu1–X1	104.64(6)	101.2	106.78(9)	102.6
N2–Cu1–O1	88.75(8)	88.19	88.58(13)	87.55
N2–Cu1–S1	86.55(6)	84.32	86.44(10)	84.02
N2–Cu1–X1	159.91(7)	162.4	156.25(11)	159.9
O1–Cu1–S1	175.11(6)	173.9	175.02(10)	173.5
O1–Cu1–X1	92.12(7)	94.07	92.68(11)	94.12
S1–Cu1–X1	91.83(3)	91.07	91.87(5)	91.66

chelate rings and the angles between Cg(1) and Cg(2) is 85.00(8)°, Cg(1) and Cg(3) is 72.85(10)°, and Cg(2) and Cg(3) is 12.92(10)° in **1**, while the same angles in **2** are 83.78(14)°, 70.65(16)°, and 13.65(16)° (where Cg is the centroid of the ring). The chelate bite angles, \angle N1–Cu1–S1, \angle N2–Cu1–S1, and \angle N2–Cu1–O1, are 81.38(5)°, 86.55(6)°, and 88.75(8)°, respectively, in **1** and 81.76(10)°, 86.44(10)°, and 88.58(13)°, respectively, in **2**.

In the crystal structures of the complexes, there are Cl/Br...H and O...H hydrogen bonding and form a 1D supramolecular chain (figure 3 and figure S1). In **1**, Cl1 forms H-bonding with H6B with a bond distance of 2.72 Å (table S1). In addition, there is H-bonding interaction between O2 with H6A and H8 atoms with hydrogen bond distances 2.48 and 2.49 Å, respectively. The H bond interactions in **2** are very similar to **1** and details of potential H bonds are given in table S2. In addition to intermolecular H-bonding in the complexes, there are strong π – π interactions between pyridyl rings, as evident from long Cg–Cg distances compared to their respective perpendicular distances. The supramolecular

Figure 3. Supramolecular 1D chain of **1** formed by intermolecular H bonding.

1D chain formed by intermolecular H-bonding and π - π interaction between the pyridines are shown in figure 4 and figure S2, respectively, for **1** and **2** with Cg-Cg distances 3.6329 (17) and 3.723(4) for **1** and **2**, respectively.

3.3. DFT calculation and electronic spectra

For better understanding of electronic structures, DFT calculations have been performed for **1** and **2**. The full geometry optimizations for the compounds have been carried out at the DFT/UB3LYP level. Some selected optimized bond parameters for **1** and **2** are given in table 2. The optimized bond lengths and angles well reproduced the X-ray data of the complexes. Contour plots of some selected molecular orbitals are shown in figures S3 and S4 for **1** and **2**, respectively. Energy and compositions of some selected molecular orbitals are given in Supplementary tables S3 and S4, respectively, for **1** and **2**.

The experimental electronic spectra in acetonitrile of the compounds are shown in figure 5. In the 250–900 nm range, **1** and **2** exhibit similar type electronic spectra in acetonitrile. Two very weak transitions at 683–686 and 527–534 nm along with two sharp peaks

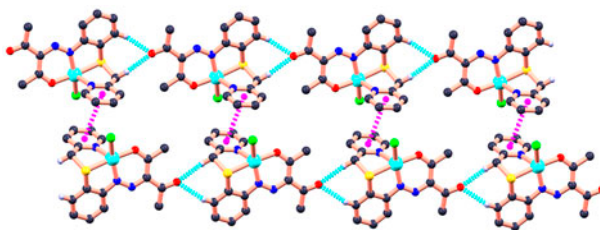


Figure 4. Supramolecular 1D chain of **1** formed by intermolecular H bonding (•••••) and π - π interaction (•••••) (see <http://dx.doi.org/10.1080/00958972.2013.857407> for color version).

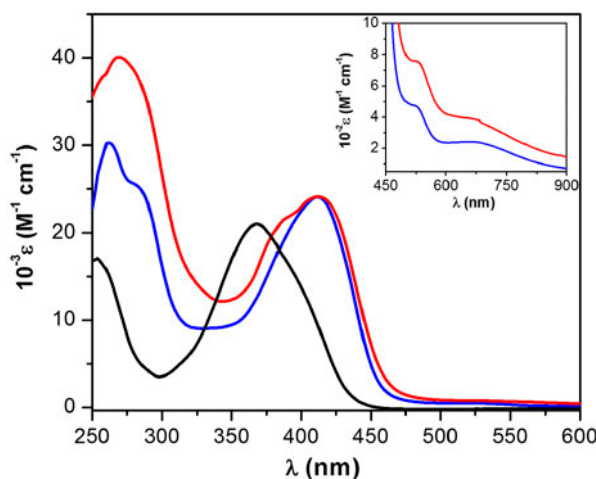


Figure 5. Electronic spectra of HL (—), **1** (—) and **2** (—) in acetonitrile (see <http://dx.doi.org/10.1080/00958972.2013.857407> for color version).

at 411–412 and 262–269 nm have been observed. To simulate the experimental electronic spectra of the complexes, TDDFT calculations have been performed in acetonitrile. Weak bands at 683–686 and 527–534 nm correspond to d–d transitions in the complexes (tables 3 and 4). The strong peak at 411–412 nm has mixed $\pi(L) \rightarrow \pi^*(L)$ (intra-ligand charge transfer transition, ILCT) and $p\pi(X) \rightarrow \pi^*(L)$ (halogen to ligand charge transfer transition, XLCT) ($X = \text{Cl}(\mathbf{1})$ and $\text{Br}(\mathbf{2})$) character. In addition, strong ligand centered bands at 262–269 nm correspond to $\pi(L) \rightarrow \pi^*(L)$ transitions in the complexes.

3.4. Electrochemistry

The electrochemical data of all the complexes obtained in acetonitrile solution using TBAP as supporting electrolyte are presented in table 5. Typical cyclic voltammogram (CV) of **1** obtained by using a *Pt*-working electrode and Ag/AgCl reference electrode is shown in figure 6. The complexes exhibit one reversible reduction couple at $-(0.024\text{--}0.032)$ V versus Ag/Ag^+ , (ΔE_p , 72–75 mV) corresponding to $\text{Cu}(\text{II})$ to $\text{Cu}(\text{I})$ reduction. In addition, irreversible oxidative and reductive responses at 0.824–0.874 and $-(1.081\text{--}1.122)$ V correspond to $\text{Cu}(\text{II})$ to $\text{Cu}(\text{III})$ oxidation and L to $L^{\cdot-}$ reduction, respectively.

3.5. Magnetic moment measurements

Magnetic moment measurements in the solid state show that the present complexes are paramagnetic at room temperature. The observed magnetic moments of these complexes are 1.75 and 1.84 BM for **1** and **2**, respectively. These values are close to the values expected for $\text{Cu}(\text{II})$ complexes [52] and is in fair agreement with the spin only system $S = \frac{1}{2}$ and characteristics of d^9 electronic configuration of $\text{Cu}(\text{II})$ in the complexes.

3.6. EPR properties

EPR spectra of **1** and **2** in acetonitrile solution at 77 K are shown in figure 7 and figure S5, respectively. Derived EPR parameters at 77 K are given in table 5. The EPR spectra of the complexes are clearly axial ($g_{\parallel} > g_{\perp} > 2.0$, $G = (g_{\parallel} - 2)/(g_{\perp} - 2) = 4.6$ and 3.1 for **1** and **2** respectively), which corresponds to $d_{x^2-y^2}$ ground state for copper(II) located in a

Table 3. Some selected vertical electronic transitions of **1** obtained in UB3LYP/TDDFT/CPCM calculation in acetonitrile.

$E_{\text{excitation}}$ (eV)	$\lambda_{\text{excitation}}$ (nm)	Osc. strength (f)	Key transitions	Character	$\lambda_{\text{expt.}}$ ($\text{M}^{-1}\text{cm}^{-1}$)
1.7379	713.43	0.0005	(53%)HOMO – 15(β) \rightarrow LUMO(β)	$d_{z^2} \rightarrow d_{x^2-y^2}$	686 (239)
2.1702	571.32	0.0087	(43%)HOMO – 12(β) \rightarrow LUMO(β) (25%)HOMO – 13(β) \rightarrow LUMO(β)	$d_{xz} \rightarrow d_{x^2-y^2}$	
2.3047	537.96	0.0042	(39%)HOMO – 14(β) \rightarrow LUMO(β) (31%)HOMO – 13(β) \rightarrow LUMO(β)	$d_{yz} \rightarrow d_{x^2-y^2}$ $d_{xz} \rightarrow d_{x^2-y^2}$	527 (469)
3.0213	410.36	0.1357	(59%)HOMO – 1(β) \rightarrow LUMO+1(β) (21%)HOMO(α) \rightarrow LUMO(α)	$\text{Cl}(p\pi) \rightarrow \text{L}(\pi^*)$ $\text{L}(\pi) \rightarrow \text{L}(\pi^*)$	411 (24,028)
3.2930	376.51	0.0686	(37%)HOMO – 2(β) \rightarrow LUMO+1(β) (27%)HOMO – 1(α) \rightarrow LUMO(α)	$\text{L}(\pi) \rightarrow \text{L}(\pi^*)$	285 (25,185)
4.2013	295.11	0.2509	(40%)HOMO – 2(β) \rightarrow LUMO+2(β) (25%)HOMO(α) \rightarrow LUMO+2(α)	$\text{L}(\pi) \rightarrow \text{L}(\pi^*)$	262 (30,386)

Table 4. Some selected vertical electronic transitions of **2** obtained in UB3LYP/TDDFT/CPCM calculation in acetonitrile.

$E_{\text{excitation}}$ (eV)	$\lambda_{\text{excitation}}$ (nm)	Osc. strength (f)	Key transitions	Character	$\lambda_{\text{expt.}}$ ($\text{M}^{-1} \text{cm}^{-1}$)
1.8018	688.12	0.0055	(57%)HOMO-15(β) \rightarrow LUMO(β)	$d_{z^2} \rightarrow d_{x^2-y^2}$	683 (376)
2.0004	619.80	0.0071	(53%)HOMO-12(β) \rightarrow LUMO(β)	$d_{xz} \rightarrow d_{x^2-y^2}$	
2.2483	551.45	0.0104	(40%)HOMO-13(β) \rightarrow LUMO(β)	$d_{xz} \rightarrow d_{x^2-y^2}$	534 (754)
			(23%)HOMO-14(β) \rightarrow LUMO(β)	$d_{yz} \rightarrow d_{x^2-y^2}$	
3.0130	411.49	0.1247	(71%)HOMO-2(β) \rightarrow LUMO+1(β)	$\text{Br}(p\pi)/\text{L}(\pi) \rightarrow \text{L}(\pi^*)$	412 (24,096)
3.2930	376.51	0.1006	(42%)HOMO-6(α) \rightarrow LUMO(α)	$\text{L}(\pi) \rightarrow \text{L}(\pi^*)$	388 (21,566)
			(25%)HOMO(β) \rightarrow LUMO+2(β)	$\text{Br}(p\pi) \rightarrow \text{L}(\pi^*)$	
4.1078	301.82	0.1606	(47%)HOMO-6(α) \rightarrow LUMO(α)	$\text{L}(\pi) \rightarrow \text{L}(\pi^*)$	269 (40,104)
			(26%)HOMO-3(β) \rightarrow LUMO+2(β)		

Table 5. Cyclic voltammetric^{a,b} and EPR^c data of **1** and **2**.

Compound	Electrochemical data			EPR data			
	$\text{Cu}^{\text{II}}/\text{Cu}^{\text{III}}$ (E_{pa} , V)	$\text{Cu}^{\text{II}}/\text{Cu}^{\text{I}}$ ($E_{1/2}$, V) (ΔE_p , mV)	L/L^{*+} (E_{pc} , V)	g_{\perp}	g_{\parallel}	A_{\parallel}	A_{\perp}
1	0.872	-0.024 (75)	-1.081	2.023	2.107	172.4	14.4
2	0.824	-0.031 (72)	-1.122	2.044	2.134	176.2	13.8

^aPt – wire working electrode; Pt – wire auxiliary electrode and Ag/AgCl reference electrode; [nBu₄N][ClO₄] supporting electrolyte; scan rate = 50 mV s⁻¹; solvent is acetonitrile.

^b E_{pc} = cathodic peak potential; E_{pa} = anodic peak potential; $E_{1/2} = \frac{1}{2} (E_{\text{pc}} + E_{\text{pa}})$ and $\Delta E_p = |E_{\text{pc}} - E_{\text{pa}}|$.

^c A_{\parallel} in 10⁻⁴ cm⁻¹.

square-based environment [53]. The g_{\parallel} (2.107 – 2.134) and A_{\parallel} (172 – 176 × 10⁻⁴ cm⁻¹) values lie in the range typical for the analogous square pyramidal copper(II) complexes [52, 54]. The values of $g_{\parallel}/A_{\parallel}$ (123 – 121 cm) for the complexes are within the range (105–135 cm) expected for copper(II) complexes with perfect square-based geometry [55]. The spin density of the complexes obtained by UB3LYP/DFT calculation also supports the $d_{x^2-y^2}$ ground state of the complexes (figure 8 and figure S6).

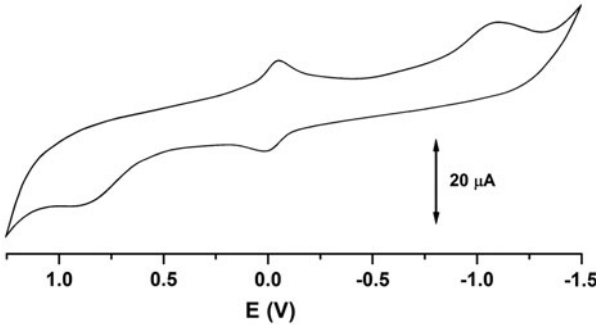


Figure 6. Cyclic voltammogram of **1** in acetonitrile.

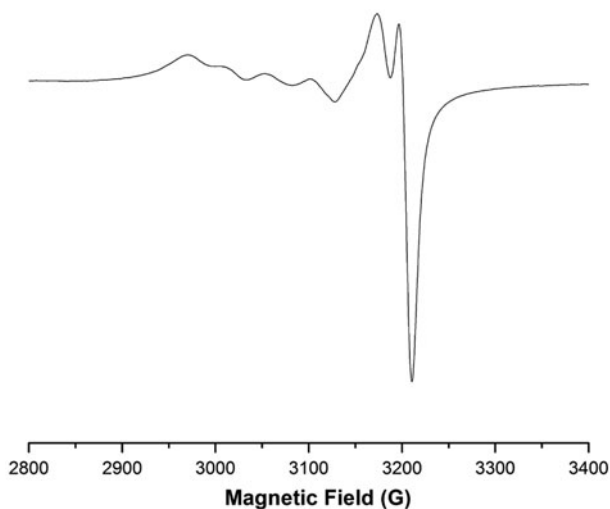


Figure 7. EPR spectrum of **1** in acetonitrile at 77 K.

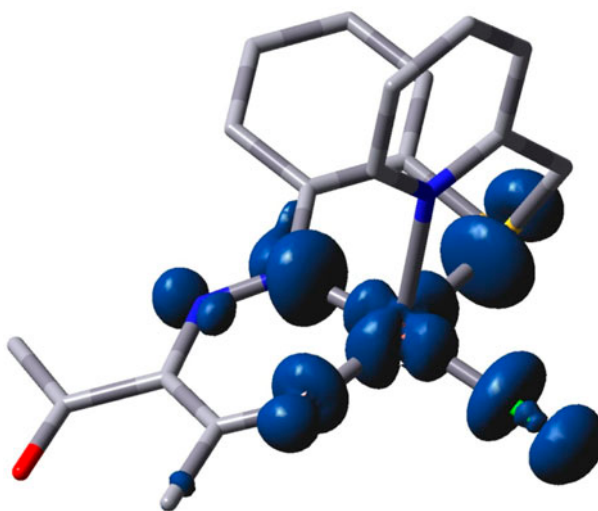


Figure 8. Spin density plot of **1** obtained in UB3LYP/DFT calculation.

4. Conclusion

Pseudo-square pyramidal Cu(II) complexes with a new N_2SO donor thioether containing arylazo ligand (HL) has been synthesized and characterized by different spectroscopic techniques abetted with DFT and TDDFT calculations. The X-ray structure and EPR spectra suggest square pyramidal geometry around Cu(II). The cyclic voltammetric study shows reversible Cu(II)/Cu(I) reduction couple along with irreversible Cu(II) to Cu(III) oxidation and L to $L^{\bullet-}$ reduction.

Supplementary material

Crystallographic data for **1** and **2** have been deposited with the Cambridge Crystallographic Data Center, CCDC No. 827403 and 827401 for **1** and **2**, respectively. Copies of this information may be obtained free of charge from the Director, CCDC, 12 Union Road, Cambridge CB2 1EZ, UK (E-mail: deposit@ccdc.cam.ac.uk or <http://www.ccdc.cam.ac.uk>).

Acknowledgement

A.K. Pramanik and M.S. Jana are very much thankful to CSIR, New Delhi, India for fellowship.

Funding

This work was financially supported by the Department of Science and Technology, New Delhi, India [grant number SR/FT/CS-73/2010].

Supplemental data

Supplemental data for this article can be accessed <http://dx.doi.org/10.1080/00958972.2013.857407>.

References

- [1] K. Krishnakutty, V.T. Rema. *Synth. React. Inorg. Met. Org. Chem.*, **25**, 243 (1995).
- [2] K. Krishnakutty, J. Michael. *J. Coord. Chem.*, **28**, 259 (1993).
- [3] M.K. Paira, T.K. Mondal, E. López-Torres, J. Ribas, C. Sinha. *Polyhedron*, **29**, 3147 (2010).
- [4] M.K. Paira, T.K. Mondal, D. Ojha, A.M.Z. Slawin, E.R.T. Tiekink, A. Samanta, C. Sinha. *Inorg. Chim. Acta*, **370**, 175 (2011).
- [5] R.A. Allred, S.A. Hufner, K. Rudzka, A.M. Arif, L.M. Berreau. *Dalton Trans.*, 351 (2007).
- [6] M.R. Malachonsk, M. Adams, N. Elia, A.L. Rheingold, R.S. Kelly. *J. Chem. Soc., Dalton Trans.*, 2177 (1999).
- [7] B. Adhikary, S. Liu, C.R. Lucas. *Inorg. Chem.*, **32**, 5957 (1993).
- [8] P. Chakraborty, S.K. Chandra, A. Chakravorty. *Inorg. Chem.*, **32**, 5349 (1993).
- [9] S. Karmakar, S.B. Choudhury, A. Chakravorty. *Inorg. Chem.*, **33**, 6148 (1994).
- [10] K. Pramanik, S. Karmakar, S.B. Choudhury, A. Chakravorty. *Inorg. Chem.*, **36**, 3562 (1997).
- [11] S. Mukhopadhyay, D. Ray. *J. Chem. Soc., Dalton Trans.*, 265 (1995).
- [12] S. Karmakar, S.B. Choudhury, D. Ray, A. Chakravorty. *Polyhedron*, **12**, 2325 (1993).
- [13] A.K. Singh, R. Mukherjee. *Dalton Trans.*, 2886 (2005).
- [14] S. Chandra, L.K. Gupta, Sangeetika. *Spectrochim. Acta, Part A*, **62**, 453 (2005).
- [15] K.P. Balasubramanian, K. Parameswari, V. Chinnusamy, R. Prabhakaran, K. Natarajan. *Spectrochim. Acta, Part A*, **65**, 678 (2006).
- [16] K.P. Balasubramanian, R. Karvembu, R. Prabhakaran, V. Chinnusamy, K. Natarajan. *Spectrochim. Acta, Part A*, **68**, 50 (2007).
- [17] T. Rosu, E. Pahontu, C. Maxim, R. Georgescu, N. Stanica, A. Gulea. *Polyhedron*, **30**, 154 (2011).
- [18] P. Sathyadevi, P. Krishnamoorthy, M. Alagesan, K. Thanigaimani, P. Thomas Muthiah, N. Dharmaraj. *Polyhedron*, **31**, 294 (2012).
- [19] K.M. Vyas, R.G. Joshi, R.N. Jadeja, C.R. Prabha, V.K. Gupta. *Spectrochim. Acta, Part A*, **84**, 256 (2011).
- [20] R. Karvembu, S. Hemalatha, R. Prabhakaran, K. Natarajan. *Inorg. Chem. Commun.*, **6**, 486 (2003).
- [21] G.D. Frey, Z.R. Bell, J.C. Jeffery, M.D. Ward. *Polyhedron*, **20**, 3231 (2001).
- [22] F. Mevellec, S. Collet, D. Deniand, A. Reliquet, J.C. Meslin. *J. Chem. Soc. Perkin Trans.*, **1**, 3128 (2001).
- [23] F. Thomas. *Eur. J. Inorg. Chem.*, **2379**, (2007).
- [24] L. Zhou, D. Powell, K.M. Nicholas. *Inorg. Chem.*, **46**, 7789 (2007).
- [25] M. Rombach, J. Seebacher, M. Ji, G. Zhang, G. He, M.M. Ibrahim, B. Benkml, H. Vahrenkamp. *Inorg. Chem.*, **45**, 4571 (2006).

- [26] L.M. Berreau. *Eur. J. Inorg. Chem.*, 273 (2006).
- [27] R.H. Holm, P. Kennepohl, E.I. Solomon. *Chem. Rev.*, **96**, 2239 (1996).
- [28] J.Y. Chen, X.X. Ren, Z.W. Mao, X.Y. Le. *J. Coord. Chem.*, **65**, 2182 (2012).
- [29] Q. Yang, S. Chen, G. Xie, S. Gao. *J. Coord. Chem.*, **65**, 2584 (2012).
- [30] L.F. Zhang, Y. Zhao, Z.H. Ni, M.M. Yu, H.Z. Kou. *J. Coord. Chem.*, **65**, 2584 (2012).
- [31] P.T. Garcia, E.V. Zahinos, F.L. Giles, A.B. Garcia. *J. Coord. Chem.*, **65**, 3556 (2012).
- [32] H.L. Zhu, W. Xu, J.L. Lin, C. Zhang, Y.Q. Zheng. *J. Coord. Chem.*, **65**, 3983 (2012).
- [33] Y.H. Yu, C.Y. Ren, G.F. Hou, H. Ye, J.S. Gao. *J. Coord. Chem.*, **65**, 4137 (2012).
- [34] J.F. Song, J. Zhang, R.S. Zhou, L. Sun, T.P. Hu, Q.L. Li. *J. Coord. Chem.*, **65**, 4375 (2012).
- [35] Z.L. Hua, W.W. Na, W. Yuan, S. Guang. *J. Coord. Chem.*, **66**, 227 (2013).
- [36] F. He, K.Z. Xu, H. Zhang, Q.Q. Qiu, J.R. Song, F.Q. Zhao. *J. Coord. Chem.*, **66**, 845 (2013).
- [37] P. Chattopadhyay, Y.H. Chiu, J.M. Lo, C.S. Chung, T.H. Lu. *Appl. Radiat. Isot.*, **52**, 217 (2000).
- [38] G.M. Sheldrick. *SHELX97, Programs for Crystal Structure Analysis*; University of Göttingen: Göttingen, (1997).
- [39] M.J. Frisch, G.W. Trucks, H.B. Schlegel, G.E. Scuseria, M.A. Robb, J.R. Cheeseman, J.A. Montgomery Jr., T. Vreven, K.N. Kudin, J.C. Burant, J.M. Millam, S.S. Iyengar, J. Tomasi, V. Barone, B. Mennucci, M. Cossi, G. Scalmani, N. Rega, G.A. Petersson, H. Nakatsuji, M. Hada, M. Ehara, K. Toyota, R. Fukuda, J. Hasegawa, M. Ishida, T. Nakajima, Y. Honda, O. Kitao, H. Nakai, M. Klene, X. Li, J.E. Knox, H.P. Hratchian, J.B. Cross, V. Bakken, C. Adamo, J. Jaramillo, R. Gomperts, R.E. Stratmann, O. Yazyev, A.J. Austin, R. Cammi, C. Pomelli, J.W. Ochterski, P.Y. Ayala, K. Morokuma, G.A. Voth, P. Salvador, J.J. Dannenberg, V.G. Zakrzewski, S. Dapprich, A.D. Daniels, M.C. Strain, O. Farkas, D.K. Malick, A.D. Rabuck, K. Raghavachari, J.B. Foresman, J.V. Ortiz, Q. Cui, A.G. Baboul, S. Clifford, J. Cioslowski, B.B. Stefanov, G. Liu, A. Liashenko, P. Piskorz, I. Komaromi, R.L. Martin, D.J. Fox, T. Keith, M.A. Al-Laham, C.Y. Peng, A. Nanayakkara, M. Challacombe, P.M.W. Gill, B. Johnson, W. Chen, M.W. Wong, C. Gonzalez, J.A. Pople. *Gaussian 03, Revision D.01*, Gaussian, Inc., Wallingford, CT (2004).
- [40] A.D. Becke. *J. Chem. Phys.*, **98**, 5648 (1993).
- [41] C. Lee, W. Yang, R.G. Parr. *Phys. Rev. B*, **37**, 785 (1988).
- [42] A.W. Ehlers, M. Bohme, S. Dapprich, A. Gobbi, A. Hollwarth, V. Jonas, K.F. Kohler, R. Stegmann, A. Veldkamp, G. Frenking. *Chem. Phys. Lett.*, **208**, 111 (1993).
- [43] R. Bauernschmitt, R. Ahlrichs. *Chem. Phys. Lett.*, **256**, 454 (1996).
- [44] R.E. Stratmann, G.E. Scuseria, M.J. Frisch. *J. Chem. Phys.*, **109**, 8218 (1998).
- [45] M.E. Casida, C. Jamorski, K.C. Casida, D.R. Salahub. *J. Chem. Phys.*, **108**, 4439 (1998).
- [46] V. Barone, M. Cossi. *J. Phys. Chem. A*, **102**, 1995 (1998).
- [47] M. Cossi, V. Barone. *J. Chem. Phys.*, **115**, 4708 (2001).
- [48] M. Cossi, N. Rega, G. Scalmani, V. Barone. *J. Comput. Chem.*, **24**, 669 (2003).
- [49] N.M. O'Boyle, A.L. Tenderholt, K.M. Langner. *J. Comput. Chem.*, **29**, 839 (2008).
- [50] A.W. Addison, T.N. Rao, J. Reedijk, J. Van Rijn, G.C. Verschoor. *J. Chem. Soc., Dalton Trans.*, 1349 (1984).
- [51] A. Valent, M. Kotiutova, O. Svajlenkova, D. Hudecova, P. Olejnikova, M. Melnik. *J. Coord. Chem.*, **57**, 1279 (2004).
- [52] P.A.N. Reddy, B.K. Santra, M. Nethaji, A.R. Chakravarty. *J. Inorg. Biochem.*, **98**, 377 (2004).
- [53] M. Vaidyanathan, R. Viswanathan, M. Palaniandavar, T. Balasubramanian, P. Prabhakaran, P.T. Muthiah. *Inorg. Chem.*, **37**, 6418 (1998).
- [54] A.W. Addison, P.J. Burke, K. Henrick, T. Nageswara Rao, E. Sinn. *Inorg. Chem.*, **22**, 3645 (1983).
- [55] U. Sakaguchi, A.W. Addison. *J. Chem. Soc., Dalton Trans.*, 600 (1979).